Available online at www.sciencedirect.com
SCIENCE DIRECT®
International Journal of Refrigeration 28 (2005) 37–50
REVUE INTERNATIONALE DU FROID
INTERNATIONAL JOURNAL OF
refrigeration
www.elsevier.com/locate/ijrefrig

The fluid dynamics of ice slurry

Andrej Kitanovski[a,*], Didier Vuarnoz[a], Derrick Ata-Caesar[a], Peter W. Egolf[a], Torben M. Hansen[b], Christian Doetsch[c]

[a]*University of Applied Sciences of Western Switzerland (UASWS)*
[b]*Danish Technological Institute (DTI), Denmark*
[c]*Fraunhofer UMSICHT Institut*

Received 11 February 2003; received in revised form 19 April 2004; accepted 16 July 2004

Abstract

A review of research work of fluid dynamics of fine-crystalline ice slurry is presented. Different rheological models which are applied are presented. Numerous models for the friction factor, obtained by empirical and semi-empirical approximation, are discussed. An overview of existing pressure drop experiments is given and problematic issues of respective measurements and experimental results are outlined. Because ice slurry is a two-phase fluid that is considered to be homogeneous, only in some cases work on stratified suspension flows is cited. Finally a variety of experimental results and some theoretical calculations of ice slurry flow patterns are shown.

Keywords: Two-phase secondary refrigerant; Ice slurry; Survey; Research; Physical property; Rheological property

Coulis de glace: dynamique des fluides

Mots clés: Frigoporteur diphasique; Coulis de glace; Enquête; Recherche; Propriété physique; Propriété rhéologique

1. Introduction

For several years researchers have been making efforts to describe the physical properties of ice slurry, its fluid dynamics and its heat transfer characteristics. Because various kinds of antifreeze depressants exist and can be used for producing ice slurry, published properties of ice slurries are always specific to a certain freeze depressing additive. Attention needs to be given to the inhibitors, which are commonly used in secondary refrigerants, and which affect basic properties like the freezing temperature. The method of producing and storing ice slurry also has a strong impact on the occurring ice slurry properties. This is particularly, because the size distribution of the ice particles varies for different production methods (e.g. vacuum generators, scraped-surface generators, generators based on super-cooling of water, etc.) The mean particle size increases with the duration of storage and mixing. A variety of flow patterns are observed in ice slurry flows. They depend on the piping system, the operation parameters and the aforementioned physical properties. If a safe operation of a system is required, the flow pattern should correspond to homogeneous flow, which implies a constant ice concentration field as a function of the cross-sectional area of the tube.

* Corresponding author. Tel.: +41-24-557-61-54; fax: +41-24-426-44-77.
E-mail address: andrej.kitanovski@eivd.ch (A. Kitanovski).

0140-7007/$35.00 © 2004 Elsevier Ltd and IIR. All rights reserved.
doi:10.1016/j.ijrefrig.2004.07.010

Nomenclature

Standard

A	area (m^2)
C	local concentration, concentration
Ca	Casson number
C_D	drag coefficient
D	pipe diameter (m)
d	ice particle diameter (m)
E_S	mass diffusion coefficient (m^2/s)
F	Fanning friction factor
He	Hedstrom number
L	length (m)
n	hindred settling parameter
p	pressure (Pa)
R	radial coordinate, specific pressure drop (Pa/m)
Re	Reynolds number
s, S	density ratio between solid and liquid
t	time (s)
T	temperature (°C)
V, v	velocity (m/s)
w	terminal settling velocity (m/s)
x	axial coordinate
y	radial coordinate

Greek

ϕ	angle of internal friction
ρ	density (kg/m^3)
σ	dispersive stress (Pa)
η	viscosity (Pa s)
ν	kinematic viscosity (m^2/s)
τ_{w0}	yield stress (Pa)
τ_w	wall stress (Pa)
τ	yield stress (Pa)
λ	Darcy's friction factor, thermal conductivity (W/mK)

Subscripts

app	apparent
B	Bingham
C	Casson
crit	critical
d	delivered
eff	effective
i	internal
f	fluid
is	ice slurry
K	arbitrary constant
l, L	liquid
max	maximum
n	power index
p	particle
r	in-situ
S,s	solid
v	volume, in-situ
0	limiting viscosity at zero shear rate

2. Rheology

Homogeneous suspensions are frequently described as single-phase, isotropic fluids with modified rheological behaviour. Instead of the viscosity of the liquid, η_L, a modified so called 'effective viscosity' of the suspension, η_{eff}, is commonly introduced. Many different models have been proposed for the viscosity of suspensions. Most of them essentially extend the work of Einstein ($C<0.01$) [1]:

$$\eta_{eff} = \eta_L(1 + 2.5C) \tag{1}$$

In this equation C is the concentration of the solid phase in a solid-liquid mixture. Eq. (1) does not take the sizes or positions of the particles into account, and the theory neglects the effects of particle interaction. Several models for the viscosity of Newtonian suspensions have been developed, as presented, e.g. in Ref. [2]. One of the most frequently applied equation for the viscosity of suspensions, which takes not only the concentration of the solid phase, but also the interaction between the solid particles into consideration, was given by Thomas [3]:

$$\eta_{eff} = \eta_L(1 + 2.5C + 10.05C^2 + 0.00273\exp(16.6C)) \tag{2}$$

The model is valid for particle concentrations up to 62.5% and particle sizes ranging from 0.1 to 435 μm. It considers that the flow is homogeneous. Eq. (2) has been widely recognized by researchers studying ice slurries. However, as has been shown by Hansen [4], this equation over predicts the viscosity of ice slurry at ice concentrations beyond 15%. He introduced Jeffrey's [2] equation with a constant $A=4.5$ to get the best fit with experimental results. At the same time Frei and Egolf [5] observed a time-dependent behaviour of ice slurry, which results in an altering size of the ice particles and consequently in also altering viscosities. Later, Hansen et al. [6] reported on the ice particle size distribution of ice slurry. They observed an increase of the mean diameter of the particles at constant ice concentration. As a consequence the number of ice particles decreases.

Various experiments have been performed to determine the effective viscosity of ice slurries. Different experimental methods and different storage tank sizes led to significant deviations between the obtained results (see Fig. 1). Eqs. (1) and (2) describe the viscosity of Newtonian suspensions, for which the shear stress is described by:

$$\tau = \eta_{eff}\frac{dv}{dy} \tag{3}$$

If the concentration of solid particles in a suspension is high,

then the flow shows non-Newtonian behaviour and the viscosity is a function of the shear velocity. When the rheological behaviour (or model) of a particular suspension is not known, it may be useful to determine the apparent viscosity:

$$\tau = \eta_{\text{app}} \frac{\mathrm{d}v}{\mathrm{d}y} \tag{4}$$

In this equation η_{app} is a function of the shear velocity. The rheology of a suspension is approximated by a particular model. Such models are e.g. presented in Table 1.

To construct a rheogram for a particular suspension, the shear rate at the wall must be known. It may be determined by applying experimental data together with the Rabinowitch [8]–Mooney [9] equation:

$$\left.\frac{\mathrm{d}v}{\mathrm{d}y}\right|_w = \frac{8v}{D}\left[\frac{3}{4} + \frac{1}{4}\frac{\mathrm{d}\left(\ln\frac{8v}{D}\right)}{\mathrm{d}\left(\ln\frac{\Delta pD}{4L}\right)}\right] \tag{9}$$

A plot of shear stress versus shear velocity at the wall shows, which rheological model could be a candidate for a successful application. The 'yield stress' and 'viscosity' presented in Table 1 should not be interpreted as real physical properties. They are only parameters of rheological models, which are applied to get a best fit to experimental results.

2.1. A brief state of the art of ice slurry rheology

Various rheological models have been applied to describe ice slurry behaviour. Sasaki [10] considered ice slurry to be a dilating (shear thickening) power law fluid. Later, Frei and Egolf [5] proposed to apply a modified Bingham model to the flow of ice slurries, which was originally given by Papanastasiou [53]. The Bingham model was considered by several authors [11,12]. Experiments

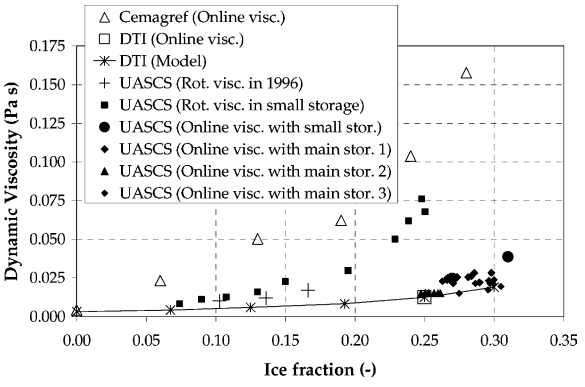

Fig. 1. Eight different series of measurements of the effective viscosity, performed at CEMAGREF, Danish Technological Institute (DTI) and the University of Applied Sciences of Central Switzerland (UASCS) with rotary and online viscometry [5]. One curve shows calculated results of a model presented by Christensen et al. (see Ref. [7]).

Table 1
Some different rheological models for laminar suspension flow ([2,15,16])

Bingham	$\tau = \tau_{\text{B}} + \eta_{\text{B}} \frac{\mathrm{d}v}{\mathrm{d}y}$	(5)
Power Law (Ostwald-de-Waele)	$\tau = K\left(\frac{\mathrm{d}v}{\mathrm{d}y}\right)^n$	(6)
Casson (1959)	$\tau^{0.5} = (\tau_{\text{C}})^{0.5} + \left(\eta_{\text{C}} \frac{\mathrm{d}v}{\mathrm{d}y}\right)^{0.5}$	(7)
Herschel–Bulkley (1987)	$\tau^n = (\tau_0)^{n_1} + K_1\left(\frac{\mathrm{d}v}{\mathrm{d}y}\right)^{n_2}$	(8)

with ice slurry have shown that for low ice concentrations it behaves like a Newtonian fluid and for high ice concentrations like a non-Newtonian fluid. It was notified that in the second case additional yield stress appears. Lakhdar [54] and later Guilpart et al. [13] used the Oswald type power law model to describe the behaviour of ice slurry with an ethanol–water (11% initial ethanol concentration) as carrier fluid:

$$\eta_{\text{app}} = \frac{\tau}{\left(\frac{\mathrm{d}v}{\mathrm{d}y}\right)} = K(C)\left(\frac{\mathrm{d}v}{\mathrm{d}y}\right)^{n(C)-1} \tag{10}$$

where:

$$n(C) = 0.263 + \frac{0.737}{1 + \left(\frac{C}{0.112}\right)^{8.34}} \quad 0 < C_r < 0.28 \tag{11}$$

$$K(C) = \mathrm{e}^{(-5.441+832.4C^{2.5})} \quad 0 < C_r < 0.13 \tag{12}$$

$$K(C) = \mathrm{e}^{(-6.227+16.487C^{0.5})} \quad 0.13 < C_r < 0.28 \tag{13}$$

A model proposed by Christensen et al. [12] describes ice slurry as a Bingham fluid. In this case the viscosity of ice slurry is defined with the Thomas equation, Eq. (2), and the yield stress is determined from experimental data:

$$\tau_0 = 0.00059C^3 - 0.00701C^2 + 0.087C - 0.02498 \tag{14}$$

Later the following approach was proposed by Jensen et al. [11]:

$$\tau_0 = \exp(a_1 + b_1 x_0^2 + c_1 C) \tag{15}$$

In this equation C denotes the ice concentration, x_0 the initial ethanol concentration (5, 10 and 20%) and the coefficients are $a_1 = -1.47$, $b_1 = 0.0035$ and $c_1 = 0.116$.

Contrary to other researchers, Doetsch [14] has given preference to the Casson model. He based his experiments on numerous kinds of freeze depressing additives. Due to this, his model approach applies for a wide range of carrier fluids. The parameters were determined as a function of the viscosity of the carrier fluid and the ice concentration (see Fig. 2).

A very appropriate rheological model for ice slurry is the one proposed by Papanastasiou [53], which allows a description of the shear rate in the entire domain with one simple equation (Fig. 3):

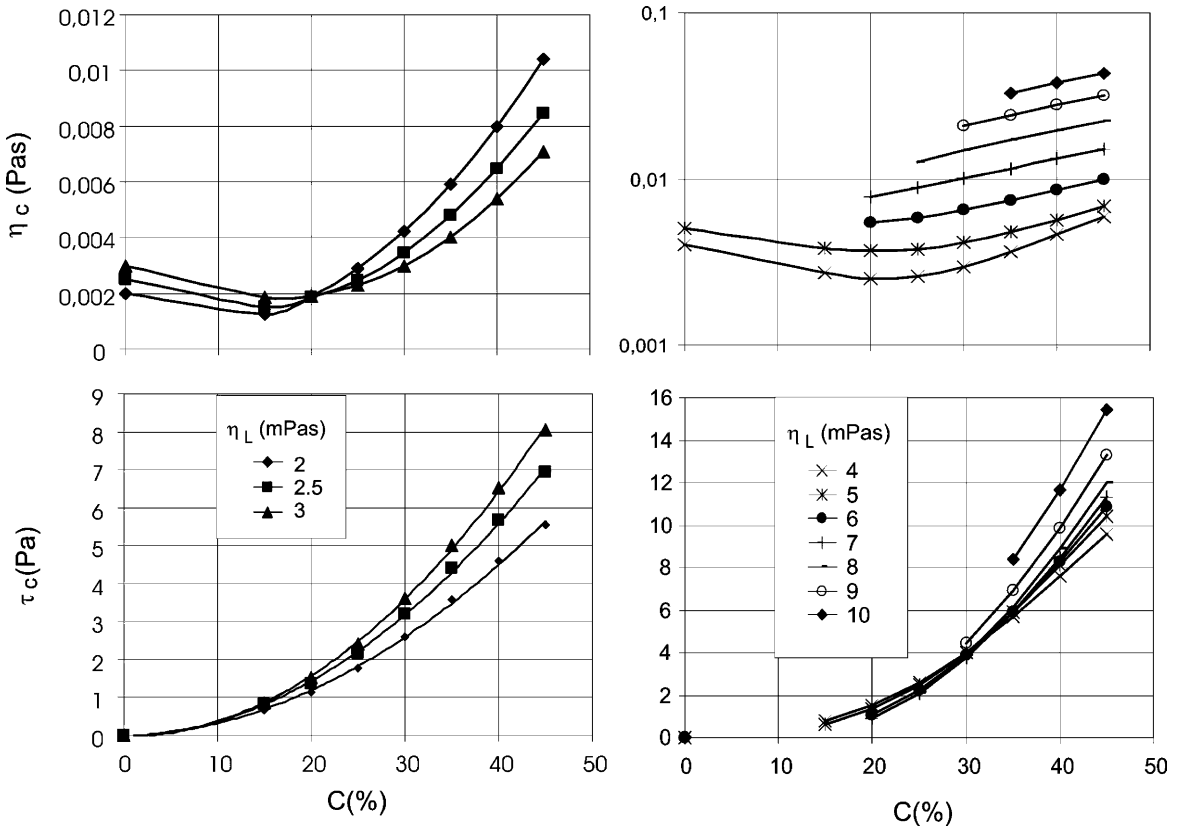

Fig. 2. Casson parameters, η_C and τ_C, as a function of the ice particle concentration (0–45%) [14] and for various viscosities of the carrier fluid (2 mPa s $<\eta_L<$ 10 mPa s).

$$\tau = \eta_{\text{app}} \frac{\partial v}{\partial r} = \tau_0(1 - \mathrm{e}^{-m(\partial v/\partial r)}) + \eta_0 \frac{\partial v}{\partial r} \tag{16}$$

If τ_0 is zero, Newtons shear rate relation (with the correct dynamic viscosity η_0) is obtained. This is also the case for the time constant $m=0$. For m approaching infinity, the description of the ideal Bingham fluid occurs as a second special case. Although the formula is empirical, it shows a convenient mathematical structure and two correct special cases.

3. Pressure drop

The most frequently applied rheological model to describe the movement of ice slurry is the Bingham model. For such a fluid—in cylindrical coordinates—the basic transport equations (from Ref. [37]) are listed in the following:(A) Continuity equation:

$$\frac{\mathrm{d}\rho}{\mathrm{d}T}\frac{\partial T}{\partial t} + \rho\frac{\partial v}{\partial x} + \frac{\partial \rho}{\partial T}\frac{\partial T}{\partial x}v = 0 \tag{17}$$

(B) Momentum equation:

$$\rho\frac{\partial v}{\partial t} + \rho v\frac{\partial v}{\partial x} + \frac{\partial p}{\partial x} - \frac{\mathrm{d}\tau_{\mathrm{B}}}{\mathrm{d}T}\frac{\partial T}{\partial r} - \eta_{\mathrm{B}}\frac{\partial^2 v}{\partial r^2} - \frac{\eta_{\mathrm{B}}}{r}\frac{\partial v}{\partial r} - \frac{\mathrm{d}\eta_B}{\mathrm{d}T}\frac{\partial T}{\partial r}\frac{\partial v}{\partial r} - \frac{1}{r}\tau_{\mathrm{B}} = 0 \tag{18}$$

(C) Energy equation:

$$\rho c_{\mathrm{p}}\frac{\partial T}{\partial t} + \rho c_{\mathrm{p}} v\frac{\partial T}{\partial x} - k\frac{\partial^2 T}{\partial r^2} - \frac{\mathrm{d}k}{\mathrm{d}T}\left(\frac{\partial T}{\partial r}\frac{\partial T}{\partial r}\right) - \frac{k}{r}\frac{\partial T}{\partial r} + \frac{T}{\rho}\frac{\mathrm{d}\rho}{\mathrm{d}T}\frac{\partial p}{\partial t} + v\frac{T}{\rho}\frac{\mathrm{d}\rho}{\mathrm{d}T}\frac{\partial p}{\partial x} = 0 \tag{19}$$

In these equations inner derivatives of the temperature were taken into consideration, but not those related to the ice concentration. Therefore, these equations are only valid, if the ice concentration is a unique function of the temperature. If this is not the case, the equations must be generalized.

3.1. Isothermal, steady, homogenous flow of ice slurry

A steady isothermal and homogenous ice slurry flow

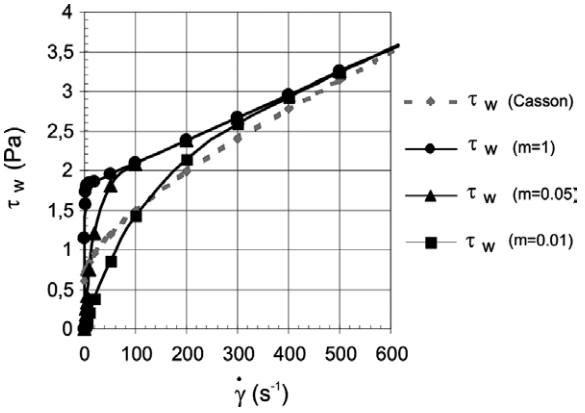

Fig. 3. Wall shear stress versus shear velocity for an ice slurry with 20% ice concentration and an initially 10% propylene glycol–water solution. Values from the modified Bingham model, Eq. (16), are compared to those from a Casson model, which was developed with experimental data from Doetsch [14].

represents the most ideal case. Then the temperature is constant, and it is therefore not necessary to consider the energy Eq. (19). Then it is advantageous to calculate the pressure drop with the Darcy–Weissbach equation:

$$\Delta p = \lambda \frac{L}{D} \frac{\rho v^2}{2} \tag{20}$$

The quantity λ denotes the friction factor. It is calculated by taking semi-empirical or empirical models into consideration (see e.g. Table 2).

To characterize the transition between laminar and turbulent flow, a known criterion for Newtonian fluids is that laminar flow is retained if $Re < 2100$ and that a transition usually occurs between $2000 < Re < 3000$. Hanks (reported by Steffe [16]) proposed the following formula for the laminar-to-turbulent transition of a Bingham fluid:

$$\mathrm{Re}_{\mathrm{crit}} = \left(\frac{\rho v D}{\eta_{\mathrm{B}}}\right) = 2100\left[1 - \frac{4}{3}\alpha + \frac{1}{3}\alpha^3\right](1-\alpha)^{-3} \tag{21}$$

In this equation the coefficient α is determined with:

$$\frac{\alpha}{(1-\alpha)^3} = \frac{\mathrm{He}}{16800} \tag{22}$$

This criterion may also be applied to other models, as for example to the Casson model. In Fig. 4 the dependence of the critical Reynolds number on the Hedström number is shown, which was calculated with Eqs. (21) and (22).

To describe the turbulent flow of a Bingham fluid, the friction factor is calculated with a relation, which was published by Govier and Aziz (reported by Steffe [16]):

$$\frac{1}{\sqrt{\lambda}} = 2.265 \log_{10}\left(1 - \frac{\tau_{\mathrm{B}}}{\tau_{\mathrm{w}}}\right) + 2.265 \log_{10}(\mathrm{Re}_{\mathrm{B}}\sqrt{\lambda}) - 1.832 \tag{23}$$

or another formula given by Darby [2] for $\mathrm{He} > 1000$:

$$\lambda = (\lambda_{\mathrm{L}}^m + \lambda_{\mathrm{T}}^m)^{1/m} \tag{24}$$

In this geometrical average λ_{L} may be calculated by applying an equation from Table 2 and the component of Eq. (24), describing the turbulent fraction, is determined by:

$$\lambda_{\mathrm{T}} = \frac{4 \times 10^a}{\mathrm{Re}_{\mathrm{B}}^{0.193}}$$

$$a = -1.378[1 + 0.14\exp(-2.9 \times 10^{-5}\mathrm{Re}_{\mathrm{B}})] \tag{25}$$

$$m = 1.7 + \frac{40000}{\mathrm{Re}_{\mathrm{B}}}$$

An investigation of Ref. [17] reveals that Eq. (23) can also be applied in combination with the Casson model.

3.2. A state of the art of pressure drop determination

Previous investigators did not consider rheological models as a basis for the determination of friction factors for laminar or turbulent flows of ice slurries. Usually only empirical correlations were developed and applied. Snoek [18] did not find large differences between the pressure drop of water and that of ice slurry with 10% ice concentration. However, at higher ice concentrations higher-pressure drops resulted. Experiments [18] revealed a minimal pressure drop in a velocity range, where the transition between heterogeneous flow and a flow with a moving bed occurred. Winters and Kooy (as reported by Snoek [18]) investigated the pressure drop of ice slurry with velocities higher than 3 m/s and with ice concentrations larger than 20%. Their experimental results show small differences in pressure drop of an ice slurry flow compared to that of flowing water. However, at velocities below 1 m/s, higher pressure drops were obtained with ice slurry, than with water. Larkin and Young (as reported by Snoek [18]) as well as Sellgren [19] noticed that the friction factor of ice slurry with ice particles of 1.2 cm diameter, 15% ice concentration and velocities between 1 and 1.5 m/s, was close to that of pure water. For

Table 2
Friction factors for laminar flow of Bingham, Power law and Casson fluids (Darby [2])

Bingham	$\lambda = \frac{64}{\mathrm{Re}_{\mathrm{B}}}\left[1 + \frac{He}{6\mathrm{Re}_{\mathrm{B}}} - \frac{He^4}{3\lambda^3\mathrm{Re}_{\mathrm{B}}^7}\right]$ with $\mathrm{He} = \frac{D^2\rho\tau_{\mathrm{B}}}{\eta_{\mathrm{B}}^2}$
Power law	$\lambda = \frac{64}{\mathrm{Re}_0}$ with $\mathrm{Re}_0 = \frac{v^{(2-n)}D^n\rho}{K}\frac{1}{8^{n-1}\left(\frac{1+3n}{4n}\right)^n}$
Casson	$\lambda = \frac{64}{\mathrm{Re}_{\mathrm{C}}}\left[1 - \frac{\mathrm{Ca}}{6\mathrm{Re}_{\mathrm{C}}} + \frac{(2\lambda\mathrm{Ca})^{0.5}}{7} + \frac{\mathrm{Ca}^4}{21\lambda^3\mathrm{Re}_{\mathrm{C}}^7}\right]$ with $\mathrm{Ca} = \frac{D^2\rho\tau_{\mathrm{C}}}{\eta_{\mathrm{C}}^2}$

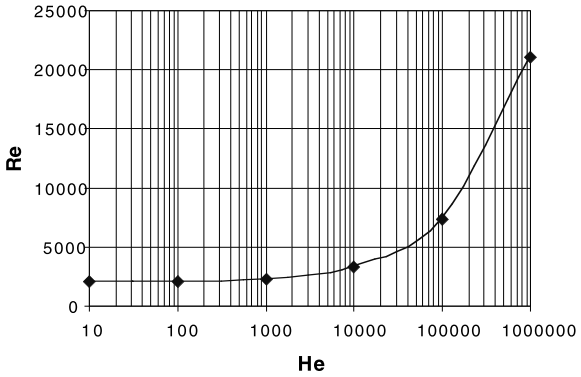

Fig. 4. Critical Reynolds number as a function of the Hedstrom number Eqs. (22) and (23).

lower velocities Sellgren [19] found a separation of the two phases and an increase of pressure loss. Larkin and Young (reported by Snoek [18]) performed experiments with ice concentrations in the range of 0–25%, but did not observe a substantial increase in pressure drop. At higher velocities though, the pressure drop was found to rapidly increase. They also found a separation of the two phases at lower velocities. Knodel (as reported also by Snoek [18]) observed a smaller pressure drop at higher ice concentration. In this case the ice slurry contained ice particles of characteristic diameters between 3 and 6 mm, the velocities varied between 1.5 and 3.5 m/s and the ice concentration was 0–15%. Takahashi [20] performed experiments with ice slurry consisting of pure water and crushed ice of 12.5 mm average particle size and an ice concentration of 25%. The results show higher pressure drop for the flow of ice slurries compared to pure water flow. At high velocities the pressure drop of the ice slurry was even lower than that of water. This is explained with a drag reducing effect with increasing velocity. Early investigations show large differences in experimental data.

Frei and Egolf [5] were the first who have observed that the pressure drop in ice slurry flow alters with time. Even when the occurrence of a supercooled or preheated carrier fluid is avoided, the pressure drop decreases with time toward an asymptotic value. Later this phenomenon was explained by different physical mechanisms, e.g. agglomeration, Ostwald rippening, etc.

In recent years numerous researchers performed experiments on pressure drop of ice slurry flow. Their valuable work has been published in Refs. [4,5,14,17,21–31] and numerous others. Some of them published empirical equations. Others worked out semi-empirical equations, which are based on rheological models, mostly of Bingham or Casson type.

Even in recent experiments on pressure drop determination and despite that the suspension was produced in identical types of ice slurry generators, very large differences in the results are observed. Frei and Egolf [5] demonstrate this in a figure comparing pressure drop measurements obtained in different laboratories. There are many reasons for these differences; one reason is a temporal variation of the ice slurry consistency (varying particle size), another is the different occurring flow patterns (homogeneous or heterogeneous flow), or then differences in the carrier fluid properties, the occurrence of a preheated or superheated carrier fluid, geometrical parameters, and the application of different measuring principles, etc. For a long time the influence of a small amount of corrosion inhibitor fluid on the physical properties of ice slurry was underestimated.

3.3. Friction factor of laminar flow

Friction factors for laminar flow of ice slurries are determined by applying equations shown in Table 2. The friction factor depends on the rheology of the fluid and hence the rheological model applied to describe the flow behaviour. Therefore, each parameter of a particular model must be determined by taking experimental material and the Rabinowitch–Mooney equation, Eq. (9), into consideration. But this method requires a large set of experimental data in order to prevent large uncertainties in the correlations of the viscosity and the yield stress. It may be that even pure empirical models lead to better results.

3.4. Semi-empirical correlations for friction factors of turbulent flow

A semi-empirical correlation is based on taking account of the rheological properties of a particular fluid and also by introducing information from measurements. For ice slurry flow Doetsch [14] introduced a new correlation, based on the Casson model. A similar equation was also proposed by Thomas (reported by Wasp [32]) for non-Newtonian fluids:

$$\lambda = 0.34179(\mathrm{Re_C})^{-0.25793}(\mathrm{Ca}+1)^{0.013532} \quad (26)$$

Eq. (26) is valid for $Re_{crit.} < Re_C < 40{,}000$ ($0 < \mathrm{Ca} < 100{,}000$) and is applicable to a wide range of ice slurries with different freeze depressing additives. Rheological parameters, obtained by modelling with the Casson fluid approach for different additives, are presented in Chapter 1.

Kitanovski [17] applied the Casson and the Bingham model to find out, which method fits best to the experimental data of Hansen. The yield stress parameter and the viscosity were determined for both models taking the Mooney–Rabinowitch equation into consideration, see Eq. (9). Jensen et al. [23] also applied the experimental data of Hansen but introduced the Thomas [3] equation into their study to determine the Bingham viscosity. For a Casson fluid Kitanovski's [17] procedure led to good agreement with Doetsch's [14] results, while Jensen's data fitted with a 20% accuracy 80% of the experimental data. Kitanovski obtained a fit with a higher accuracy, namely $\pm 15\%$ for the entire set

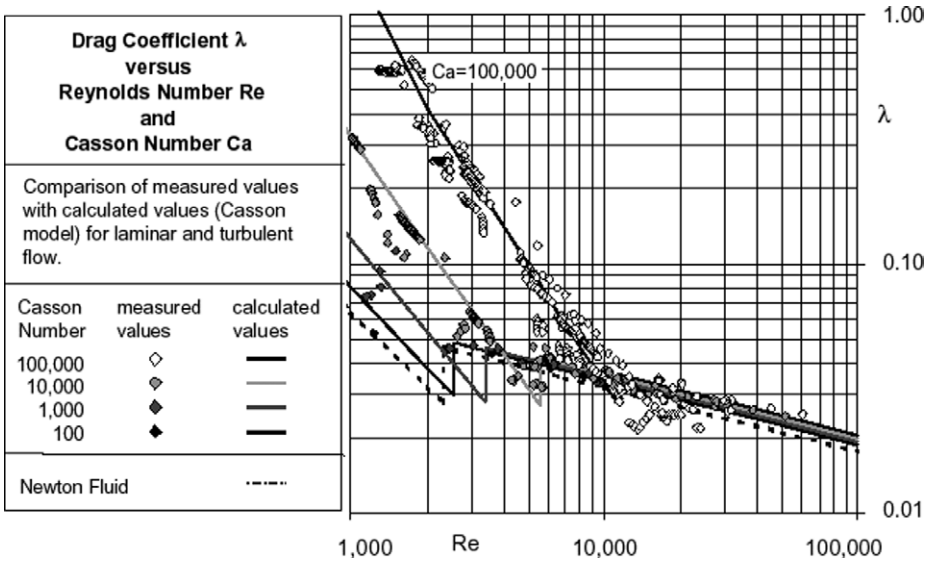

Fig. 5. Darcy's friction factor versus Reynolds number for a set of Casson numbers in the case of laminar and turbulent flow [14].

of experimental data for a Bingham fluid and ±30% for all experimental data for a Casson fluid.

Doetsch [14] obtained a maximal deviation of 5% for Ca < 1000, of 10% for 1000 < Ca < 10,000 and 20% for Ca > 10,000. From these accuracies it is concluded that at present his equation yields the best results for turbulent ice slurry flow produced with a wide variety of freeze depressing additives. However, his equation is limited to slurries with ice particle sizes between 0.1 and 0.5 mm and to isothermal homogeneous flows. Fig. 5 shows Darcy's friction factor, which was determined by Doetsch [14].

3.5. General empirical determination of the friction factor

A general empirical determination of the friction factor of an ice slurry flow is based on a dimensionless analysis. Results obtained by this method agree much better with experimental data than those extracted from semi-empirical models. In this subchapter only correlations, which are applicable to laminar or turbulent flow, are presented (see Tables 3–5).

3.6. Pressure drop in heat exchangers

The pressure drop of ice slurry in a heat exchanger must be determined considering the effects of the heat transfer, which induces a melting of ice particles. This causes an alteration of the physical properties of the ice slurry. Semi-empirical work on this subject was performed by Egolf et al. [31]. They propose an approximation to determine the average pressure drop during a steady-state transport of ice slurry through a cylindrical heat exchanger:

$$\bar{R} = \frac{R_{\text{in}}}{\ln \frac{R_{\text{in}}}{R_{\text{out}}}} \left(1 - \frac{R_{\text{out}}}{R_{\text{in}}}\right) \tag{27}$$

In this formula R denotes the specific pressure drop as a function of the ice slurry properties at the inlet, R_{in}, and the

Table 3
Empirical correlations for determining friction factors for ice slurry flow

Performed by (year)	Specification of experiment	Equation	Uncertainty
Kitanovski [17] (Experimental data from Hansen–DTI)	Plastic ABS pipe. Inner diameters 12.8, 21, 27.7 mm $v = 0.5$–2 m/s $C_r = 0$–30% Initial ethanol concentration: 5, 10, 20%	$f_{\text{is}} = f_f + b_1 C_r^{b_2} f_f^{b_3} C_D^{b_4} \left(\frac{v^2}{Dg\lvert s-1\rvert}\right)^{b_5}$ $f_f = \frac{0.0791}{\text{Re}^{0.25}}$ $\Delta p = 2f \times \frac{L}{D}\rho v^2$	±15% within 100% of all experimental data
Based on Turian's work	$d_p \sim 300$ μm Ice generator: scraper type	Coefficients presented in Table 4	
Snoek and Gupta [18]	Pipe diameters 38–100 mm $v = 0.96$–3.53 m/s $C_r = 0$–31% Initial glycol concentration 9.6–12.9% d_p—not known Ice generator: scraper type	$\Phi^2 = \frac{\lambda_{\text{is}}}{\lambda_{\text{water}}}$ $\Phi^2 = 1 + aC_{\text{r}}^b(\text{Re}_{\text{is}})^c + \text{d}C_{\text{r}}^e D^f$ $\lambda_{\text{water}} = \frac{0.316}{\text{Re}_{\text{water}}^{0.25}}$ $\Delta p = \lambda_{\text{is}} \frac{L}{D} \frac{\rho v^2}{2}$ Coefficients presented in Table 5	±10% within 100% of all experimental data

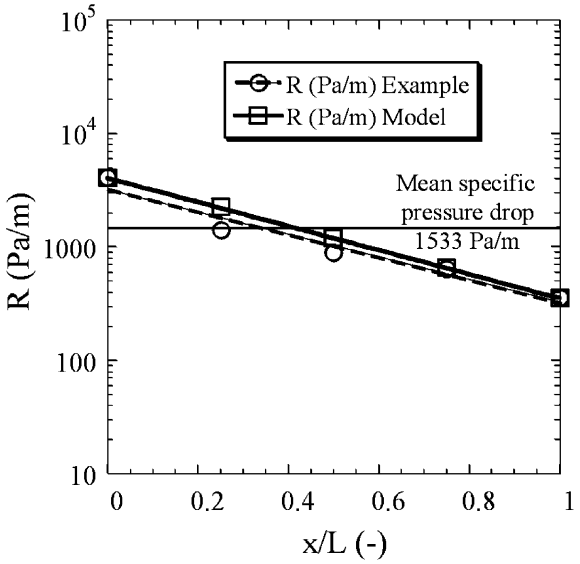

Fig. 6. The approximately exponential decrease of specific pressure drop R in a cylindrical heat exchanger. In this example R alters from the inlet to the outlet by more than a factor 10. The curve annotated Example represents a step-by-step calculation downstream in the heat exchanger. The curve annotated Model shows a result obtained with Eq. (27). Ref [31].

outlet, R_{out}, of the heat exchanger:

$$R_{in} = -\frac{dp}{dx}\bigg|_{x=0} = \frac{\lambda_{in}}{D}\frac{\rho_{in}\bar{v}_{in}^2}{2} \quad \text{and}$$
$$R_{out} = -\frac{dp}{dx}\bigg|_{x=L} = \frac{\lambda_{out}}{D}\frac{\rho_{out}\bar{v}_{out}^2}{2} \tag{28}$$

This approach assumes an exponential decrease of pressure during the transport and melting of the ice slurry along the cylindrical heat exchanger (see Fig. 6):

$$R(x) = \alpha \exp\left(-\beta\frac{x}{L}\right) \tag{29}$$

This assumption with the boundary values, Eq. (28), which determine α and β, lead to the final result (27).

Defining the average pressure drop as the arithmetic mean between inlet and outlet pressure may produce remarkably inaccurate values. In slow flow through heat exchangers, stratified or heterogeneous flow (or flow with a moving bed) may develop. This phenomenon is discussed in a following subchapter.

Various experiments have been performed to study the pressure drop of ice slurry in heat exchangers [21,23,24,30,33].

Table 5
Coefficients for an empirical correlation for initial concentration of 9.6–12.9% glycol–water solutions [18]

a	0.1119	d	0.02415
b	2.151	e	0.3996
c	0.2422	f	−0.2845

4. Flow patterns of ice slurries

To describe mathematically a heterogeneous flow of slurry the continuity, the momentum, and the energy equation are usually formulated for each component or phase. To solve these equations sophisticated numerical methods are required. For turbulent flows of suspensions two-equation turbulent models are usually applied. They take the influence of turbulent mixing into consideration. These models comprise a number of empirical coefficients and should be used cautiously. For isothermal heterogeneous flow, where the influence of heat transfer on melting and stratification may be neglected, the continuity and momentum equations are [34]:

$$\frac{\partial}{\partial t}(C_k \cdot \rho_k) + \frac{\partial}{\partial x_i}(C_k \cdot \rho_k \cdot v_{k_i}) = 0 \quad k \in \{1, 2, \ldots, m\}, \quad j \in \{1, 2, 3\} \tag{30}$$

$$C_k \cdot \rho_k \frac{Dv_{k_i}}{Dt} = C_k \cdot \rho_k \cdot g_i - \frac{\partial(C_k P)}{\partial x_i} - \frac{\partial(C_k \tau_{k_{ji}})}{\partial x_j} - R_{kl_i} - R_{k(s-k)_i} \tag{31}$$

The first Eq. (30) is the continuity equation containing the concentration of component or phase k, if the maximal number of components is m. The last two terms on the right hand side of the momentum Eq. (31) represent interaction forces (per unit volume of suspension) between component k and the (liquid) carrier fluid (l) and between component k and the component of the solid particles (s), and are not further described in detail here. All terms in Eq. (31)

Table 4
Coefficents for empirical correlations for three initial concentrations of ethanol additive, [18]

	5% Ethanol	10% Ethanol	20% Ethanol
B_1	0.00000039332	650.1835	912649.1
B_2	0.45034198847	1.147015	0.621567
B_3	4.02136479789	3.807498	3.722244
B_4	3.84746019112	1.089962	0.092936
B_5	−0.67864294281	−0.649095	−0.403264

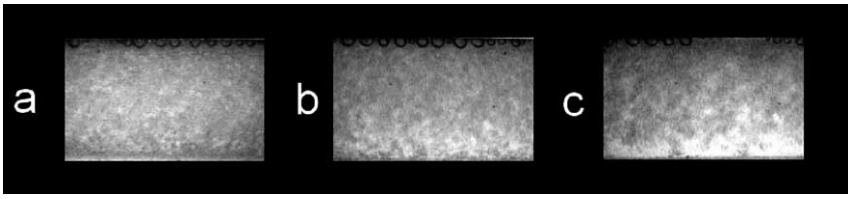

Fig. 7. Visualizations of ice slurry flows do not allow accurate distinctions of flow patterns (10% water–ethanol solution, d_p=0.2–0.4 mm, D_i=20 mm, rectangular pipe; (a) C_r=7.6%, v=0.54 m/s; (b) C_r=7.5%, v=0.23 m/s; (c) C_r=7.5%, v=0.15 m/s). Work performed by D. Vuarnoz at the University of Applied Sciences of Western Switzerland, UASWS.

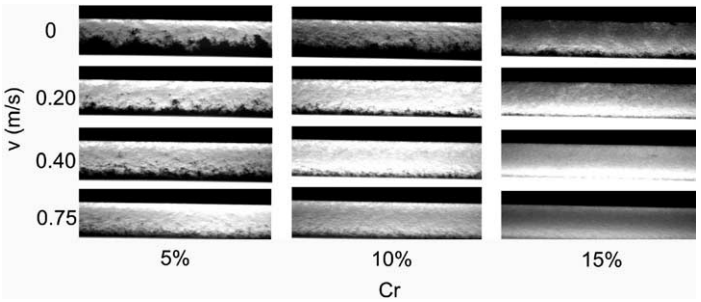

Fig. 8. Flow pattern 'diagrams' of ice slurry flow investigated at the Korean Institute of Energy Research (D_i=24 mm, 6.5% ethylene glycol–water, $\bar{d}_p$ = 0.27 mm), [26].

comprise time average and fluctuation terms. For a description of flows of ice slurries one must consider the solid particle properties, including their temporal altering shape and size. Furthermore, the slurry behaviour depends on the specific system design (pipe diameter, pipe inclination) and on the operation conditions, e.g. the forcing described by a mean cross-sectional velocity. The visualisation of ice slurry flows—for determining flow patterns—is difficult, because of the opacity of the ice slurry and in some cases because of the additional melting phenomenon. For systems design it is important to have knowledge of the parameter ranges, where different flow patterns occur. Only then stable and safe operation conditions in practical systems may be guaranteed. Moving or stationary beds must be avoided. In these cases blockage or flow pulsations in the piping system may occur, especially if the mean flow velocity is low. At least a blockage can be easily removed in an ice slurry system, namely by simply heating the pipe externally.

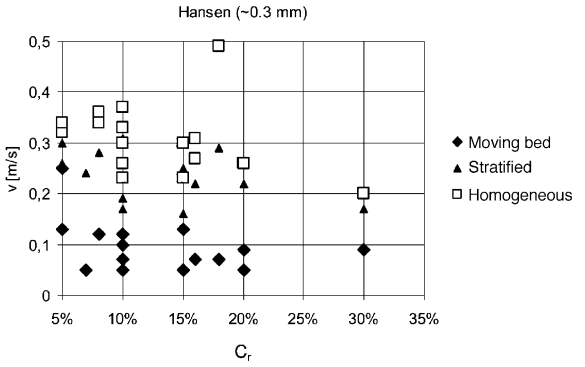

Fig. 9. Flow patterns in ice slurry flow as a function of flow velocity and ice concentration. (Work performed at DTI, DN 50, 10% water–ethanol solution).

4.1. State of the art of research on flow patterns

Research on ice slurry flow patterns began in the mid 1980s. Its objective was to acquire the necessary knowledge for providing design guidelines for ice slurry transportation systems. In early times the ice particles in the aqueous solution were produced to be relatively large, with sizes of circa 12 mm [35–37]. Nowadays ice slurry generators usually produce very small ice particles (d_p=100–300 μm). The small ice particles can be of various shapes and in some cases they agglomerate and form clusters. The properties of heterogeneous ice slurry flows differ from those of homogenous flows. Some early research work was focused on determining the friction factor of heterogeneous flow [36] and resulted in experimentally confirmed methods to calculate the velocity distributions. Because the characteristic scale of the ice particles has decreased by two orders of magnitude, new investigations are demanded to determine the physical properties and the flow parameters for all the occurring flow regimes. Among recent research in this field, which led to an improved understanding of several phenomena, are the studies on ice particle shapes and sizes and related time-dependent behaviour [5,37–39]. Other recent investigations have been focused on velocity profiles by applying numerous sophisticated experimental methods [38,40,41]. Experimental and theoretical determinations of

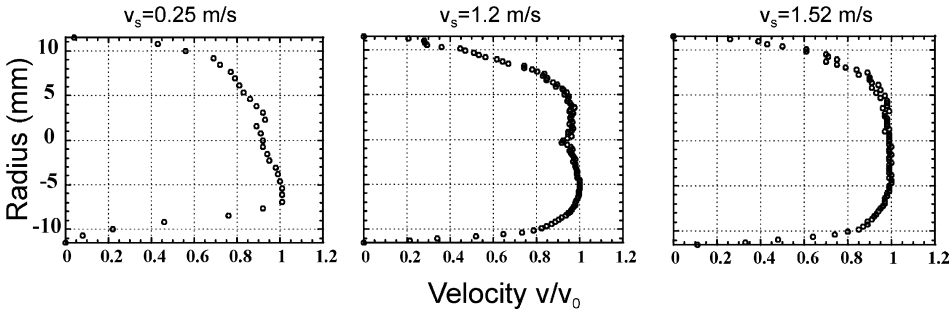

Fig. 10. Ice particle velocity profiles for an ice slurry flow (11% water–ethanol solution, $C_r = 12$, 10 and 11%, DN 25, $d_p \approx 0.1$ mm,) measured by Vuarnoz et al. [38].

the critical deposition velocities were performed by Kitanovski et al. [42]. Concentration profiles were studied by Kitanovski et al. [43] and pressure drops of heterogeneous flows were determined by Reghem [27]. Up-to-present four experiments have been performed to determine flow patterns of ice slurries [26,46], where the ice particles were small 100–300 μm. Some of the patterns were classified by simply observing the flow through a transparent wall. Such results show remarkable uncertainties, especially for close-to-homogeneous flows where a visual distinction of the small ice particle density fluctuations become difficult to carry out. Four different flow patterns have been observed: homogeneous flow, heterogeneous flow, the moving bed and the stationary bed (see Figs. 7–9).

4.2. Velocity profiles

One method to determine flow patterns is to investigate velocity profiles in cross sections of the flow. For example, the velocity profile of a laminar homogeneous ice slurry flow may be described by applying the Bingham model. However, such flow conditions are restricted to small pipe diameters with low mean velocities. The velocity of the solid phase usually differs from that of the liquid phase. This is related to the so called slip velocity, which can be neglected, if the flow is homogeneous. When the flow becomes heterogeneous the difference between the velocities of the two phases usually increases. Then the velocity in a cross section of the flow shows an asymmetric profile, i.e. the dynamic axis is lower than the axis of the pipe. Several authors have presented models for the velocity distribution in heterogeneous slurry flow, but they cannot be applied to ice slurries. Only one study [44,45] related their model to ice slurries, but the testing experiments were performed with polystyrene particles of large diameters ($d \sim 3$ mm), which is quite problematic. Among the methods to determine velocity profiles are the *U*ltrasonic *D*oppler *P*rofiler (UVP), which is an ultrasonic echography method, the Pitot tube, hot wire anemometry, and observation methods, applying high speed video cameras. The latter is not applicable to ice slurries, because of the opacity of this type of fluid. Some of the methods detect only the velocity profile of the solid or of the liquid phase. The Pitot tube can measure the velocity of the mixture, but it is very difficult to perform reliable experiments with this technique, because of blocking. Therefore, this measuring technique is only sufficiently accurate for small ice concentrations and small ice particles. Otherwise the data of Pitot tube measurements are of minor quality compared to other methods [46]. To describe the dispersion of ice particles (e.g. concentration distribution) in a slurry flow, it is convenient to use the velocity profile of the solid phase. Such measurements, which provide data of profiles of the particle velocities, were performed at the University of Applied Sciences of Western Switzerland.

For a bulk slurry velocity of 1.52 m/s axisymmetric flow conditions were observed (see in Fig. 10). When the bulk velocity is lower, e.g. $v_{\text{slurry}} = 1.2$ m/s, the dynamic axis falls slightly below the pipe axis, but the flow may still be considered to be axisymmetric. A further decrease of velocity leads to a deformed velocity profile, as can be observed in the first plot of Fig. 10, where the bulk velocity of the ice slurry was 0.25 m/s.

4.3. Concentration profiles

Analytical descriptions of the concentration distribution of ice slurry flow are mainly based on the concept of turbulent diffusion, originally given by Schmidt and Rouse [47]:

$$E_S \frac{dC}{dy} + wC = 0 \tag{32}$$

where E_S is a diffusion coefficient or a mass transfer coefficient of the solid particles and w is the terminal settling velocity of ice particles in the quiescent fluid. In Eq. (32) only the equilibrium between the net gravitational force and the lifting force due to turbulence is considered. Shook (as reported by Nasr-El-Din et al. [48]) found from his experiments (performed with high ice particle concentrations) that the concentration gradient from Eq. (32) is too low. According to Nasr-El-Din et al. [48] this can be corrected with the hindered settling multiplier, which is found in the Richardson and Zaki correlation [49]. In

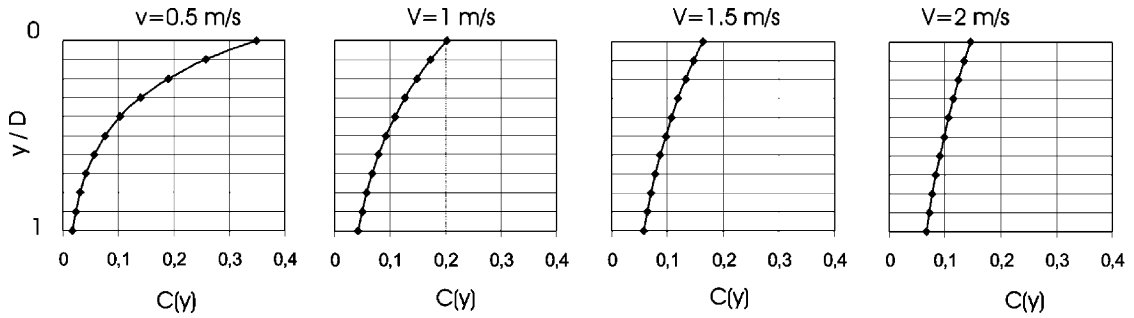

Fig. 11. Concentration profiles of ice slurry flow in a horizontal pipe (derived from Eq. (6)), ($D=27.2$ mm, $d_p=1$ mm, 10% water–ethanol solution), from Ref. [43].

Eq. (32) the interactions between the solid particles (dispersive stress) are neglected. These particle-to-particle interactions become important, as soon as the particle concentration is high or the particles are large. Bagnold [50] observed a negative slope of the concentration distribution (at the bottom of the pipe, with the maximum concentration of particles at a certain distance over the bottom) in a laminar flow of a sand suspension. A very comprehensive model was proposed by Roco and Shook [51]. The model was based on the momentum equation for the solid and the liquid phase. In this approach the differential equation for the concentration $C(y)$ is:

$$\frac{E_S^2}{w^2}\frac{\mathrm{d}^2C}{\mathrm{d}y^2}+\frac{sC}{(s-1)g\tan\phi}\frac{\partial^2(\alpha_s v_s^2)}{\partial y^2}+C^2=0 \tag{33}$$

Here v_s is the velocity distribution of the solid particles, α_s denotes the experimentally obtained turbulence coefficient and ϕ is the angle of internal friction of the dispersive stress.

The concentration distribution of the ice slurry depends on the properties of the liquid phase, the density of solid particles, the pipe diameter, the particle diameter, the shape of the ice particles, the velocity distribution of each phase, the concentration of the solid phase and the friction occurring with the transport of the slurry. These parameters essentially describe the flow patterns. It is clear that the velocity distribution is strongly coupled to the ice concentration distribution and vice versa. A simple approach—which may also be applied to describe concentration distributions in the ice slurry flow—is that of Doron [47]:

$$C(y)=C_{\max}e^{-(w/E_S)y} \tag{34}$$

According to the results of other authors [51], this equation can be successfully applied to describe ice slurry flows of small solid particle concentrations ($C_S<15\%$) (see Fig. 11):

$$C_{\max}=\frac{C_S A}{\int_A \mathrm{e}^{(-w/\varepsilon)y}\mathrm{d}A(y)} \tag{35}$$

4.4. Critical deposition velocity

The transition between flow with a moving bed and heterogeneous flow is characterised by the critical deposition velocity. Several pioneers of ice slurry research (reported by Snoek [18]) observed an increase of pressure drop when the flow velocity dropped underneath the critical deposition velocity. The observed critical velocities were high, due to the large ice particles in these early experiments. Newer experiments have shown that the critical deposition velocities are much lower than those, which have been reported by Snoek [18]. In smaller pipes there is no clear boundary between the moving and the stationary bed. The following four methods can be used for determining the deposition velocity:

(a) Evaluation of the concentration profile
(b) Evaluation of the velocity profile
(c) By observation
(d) By applying empirical correlations.

All these listed methods require experimental data. The determination with empirical correlations is the simplest approach, because it permits a fast and simple calculation of the deposition velocity. However, the estimation is less accurate than other methods. Some authors report deviations of $\pm 20\%$ [52]. The above-mentioned methods are subsequently described:

(a) A boundary condition for the concentration as a

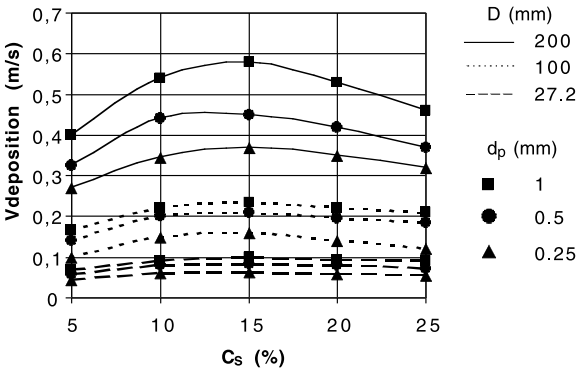

Fig. 12. Deposition velocities for ice slurry flow—theoretical model (10% water-ethanol) (Kitanovski [17]).

Table 6
The maximum packing fractions of various arrangements of monodispersed spheres [1]

Arrangement	Maximum packing fraction
Simple cube	0.52
Maximum thermodynamically stable configuration	0.548
Hexagonally packed sheets just touching	0.605
Random close packing	0.637
Face-centred cubic/hexagonal close packed	0.68
Body-centred cubic/hexagonal close packed	0.74

function of maximal radial coordinate, $C(y=D)$, is identical to the maximal concentration at the top of the pipe. When a maximum packing fraction occurs there, a moving bed starts to form. Then no further particles can be added to the top layer anymore. The maximal packing fraction is mainly determined by the geometry of the particles, as it is shown in Table 6. Authors frequently insert a packing fraction of 63% into their numerical simulation codes. However, it must be emphasised that such a concentration corresponds to stationary conditions. In the case of sedimentation processes the bed is more porous, so according to Ref. [51] additionally a dynamic factor of 0.9 should be implemented. Kitanovski [17] assumed a maximal ice packing fraction of 0.52. Furthermore Eq. (34) was applied to determine the concentration distribution of ice slurry flows.

(b) A determination of the critical deposition velocities on the basis of velocity profile evaluation is a very accurate method, but the necessary experimental procedures are complex. Fig. 12 shows the deposition velocities for different sizes, d_p, of ice particles and different pipe diameters. This theoretical model is in good agreement with the results of Hansen [39]. Additional experiments with inclined pipes would be valuable.

(c) Fig. 9 shows experimental results of ice slurry flow patterns and includes the flow pattern of a moving bed.

(d) Several different empirical correlations for suspension transport can be found in the literature [2,32,52], but they cannot be applied to ice slurry, because the constants in the equations only fit the conditions for particular experiments. A well-known empirical function was developed by Durand [32]:

$$V_{\text{deposition}} = F_L\sqrt{(2gD(S-1))} \tag{36}$$

In this equation S is the ratio between the density of the solid particles and the carrier fluid and F_L denotes a specific operating parameter as a function of particle size and concentration. Making use of experimental data from Ref. [46], Kitanovski et al. also obtained for the deposition velocity of ice slurries (DN 50, 10% water–ethanol solution, $d_p=0.1$ mm, $R^2=0.98$) the following empirical correlation for the deposition velocity:

$$\frac{V_{\text{deposition}}}{\sqrt{2gD(1-S)}} = 0.397756C_r^{0.3} \times(1-C_r)^{3.756}\left(\frac{D}{d_p}\right)^{-0.17833}\left(\frac{w\cdot 10^{-4}}{\nu_f}\right)^{-0.8383} \tag{37}$$

In this equation w represents the hindered terminal settling velocity, which has been mathematically described by different authors. The most frequently applied correlation, however, is the one derived by Richardson and Zaki [49].

Eq. (37) gives best results for small ice particles and small pipe diameters ($D_{\text{pipe}}<50$ mm), because the correlation was determined for these conditions. Furthermore, it should not be applied to extrapolate, e.g. for other ice particle and pipe diameters. As shown in Fig. 13, with increasing ice concentration, the deposition velocity increases to a finite value and then decreases again. This is the influence of the carrier fluid viscosity, which alters with higher ice concentration and influences the dynamic conditions. Similar results (when smaller particles are considered) are presented in Fig. 12.

4.5. Theoretical determination of flow patterns

A powerful method to determine flow patterns of ice slurries is the theoretical investigation of ice concentration

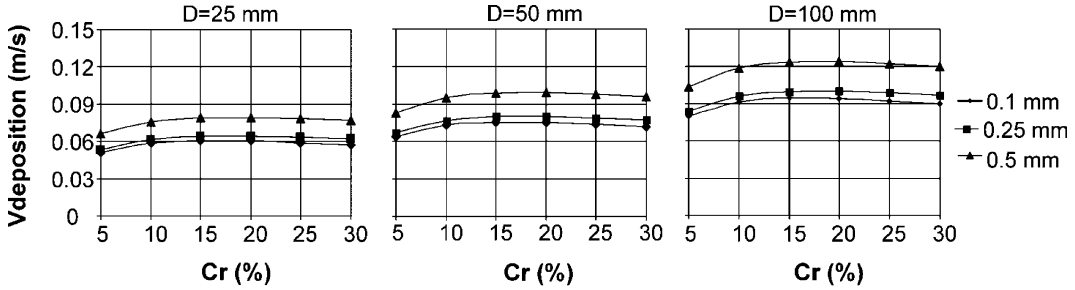

Fig. 13. Deposition velocities versus ice concentration obtained from an empirical function given by Eq. (37), [46].

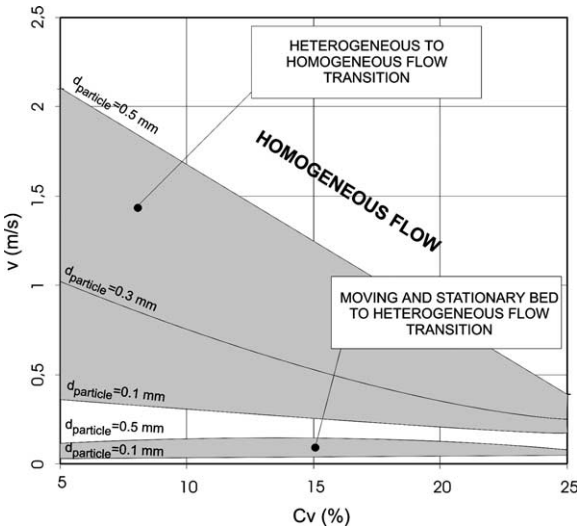

Fig. 14. Flow pattern diagram of ice slurry flows obtained by applying a theoretical model (DN 50, 10% water–ethanol solution), [46].

profiles, which—together with a defined maximal packing fraction—can provide information on whether a moving bed will develop in the flow or not. With the help of Wasp's [32] criterion for the occurrence of homogeneous flow, one can also predict the transition between heterogeneous and homogenous flow (e.g. see Fig. 14). Such results always have to be experimentally verified.

5. Conclusions and outlook

This article gives some information on the rheology, pressure drop of flows in tubes and flow patterns of ice slurries. Present results still show numerous uncertainties. Therefore, there is still much to focus on for future researchers. Some proposals for future investigations are listed bellow:

- Because of large deviations in experimental results, which were obtained in different laboratories, a further coordinated research programme on rheology of ice slurries could be advantageous. This would for example yield to clear definitions of effective physical properties.
- The effect of different particle shapes and sizes in relation to the type of ice particle production method, storage, mixing and, therefore, also of the time behaviour must be further investigated.
- The lack of sufficient experimental data sets of flow patterns, as well as a lack of numerical simulation results on stratified (isothermal and non-isothermal) ice slurry flows, makes it impossible at present to present accurate flow pattern diagrams.
- The effect of heat transfer on pressure drop and flow patterns should be also further investigated by theoreticians and experimentalists.

References

[1] H.A. Barnes, An introduction to rheology, Elsevier, Amsterdam, 1989. Chapter 7.
[2] R. Darby, Hydrodynamics of slurries and suspensions, Encyclopaedia of fluid mechanics, slurry flow technology, vol. 5 1986 Chapter 2, p. 49–92.
[3] D.G. Thomas, Transport characteristics of suspension, J Colloid Sci 1965; no. 20.
[4] T.M. Hansen, M. Kauffeld, Viscosity of ice slurry. Second Workshop on Ice-Slurries of the International Institute of Refrigeration, Paris, France.
[5] B. Frei, P.W. Egolf, Viscometry applied to the Bingham substance ice slurry. Second Workshop on Ice-Slurries of the International Institute of Refrigeration, Paris, France.
[6] T.M. Hansen, et al., Behaviour of ice slurry in thermal storage systems, ASHRAE research project RP 1166, 2002.
[7] K.G. Christensen, M. Kauffeld, Heat transfer measurements with ice slurry, International Conference of the International Institute of Refrigeration, IIR Commission B1 1997.
[8] B. Rabinowitsch, Über die Elastizität von Solen, Zeitschrift für Physikalische Chemie, A 145 (1929) 1–7.
[9] M. Mooney, Explicit formulas for slip and fluidity, J Rheol Bd 2 (1931) 210–215.
[10] M. Sasaki, T. Kawashima, H. Takahashi, Dynamics of snow-water flow in pipelines, slurry handling and pipeline transport, Hydrotransport 12 (1993) 533–613.
[11] E.N. Jensen, et al., Pressure drop and heat transfer with ice slurry, Conference of the International Institute of Refrigeration, Purdue, USA, 2000.
[12] K.G. Christensen, M. Kauffeld, Heat transfer measurements with ice slurry, International Conference of the International Institute of Refrigeration, 1997.
[13] J. Guilpart, et al., Experimental study and calculation method of transport characteristics of ice slurries, First Workshop on Ice Slurries of the International Institute of Refrigeration, Yverdon-les-Bains, Switzerland, 1999 p. 74–82.
[14] C. Doetsch, Experimentelle Untersuchung und Modellierung des Rheologischen Verhaltens von Ice-Slurries. PhD. Fraunhofer Institut-UMSICHT, Fachbereich Chemie technik der Universität Dortmund; 2001.
[15] R.W. Hanks, Principles of slurry pipeline hydraulics, Encyclopaedia of fluid dynamics, slurry flow technology, vol. 5, Gulf Publishing Company, 1986. p. 213–76.
[16] J.F. Steffe, Rheological methods in food process engineering, 2nd ed, Freeman Press, San Fransisco, CA, 1992.
[17] A. Kitanovski, PhD Thesis. University of Ljubljana, Faculty of Mechanical Engineering, Slovenia; 2003.
[18] C.W. Snoek, The design and operation of ice slurry based district cooling systems. IEA-Novem; 1993.
[19] A. Sellgren, Hydraulic behaviour of ice-particles in water, Hydrotransport , International Conference on Slurry Handling and Pipeline Transport 10 (1986) 213–217.

[20] H. Takahashi, J.W. Wilson, T. Masuyama, A laboratory study of pressure loss and pressure fluctuation for ice-water slurry flows in a horizontal pipe, Hydrotransport 12 (1993) 497–511.
[21] B.D. Knodel, et al., Heat transfer and pressure drop in ice-water slurries, J Appl Thermal Engng 20 (2000) 671–685.
[22] Chaer et al. Flow characteristics and pressure drop of ice slurries in straight tubes. Clima 2000/Napoli, World Congress, Napoli; 2001.
[23] E.N. Jensen, et al., Pressure drop and heat transfer with ice slurry, Conference of the International Institute of Refrigertion, Purdue, USA, 2000.
[24] S. Tassou, et al., Comparison of the performance of ice slurry and traditional primary and secondary refrigerants in refrigerated food display cabinet cooling coils, Fourth Workshop on Ice Slurries of the International Institute of Refrigeration, Osaka, Japan, 2001.
[25] J. Guilpart, et al., Experimental study and calculation method of transport characteristics of ice slurries, First Workshop on Ice Slurries of the International Institute of Refrigeration, Yverdon-les-Bains, Switzerland, 1999. pp. 74–82.
[26] W.I. Dong, et al., Experimental study on flow and pressure drop of ice slurry for various pipes, Fifth Workshop on Ice Slurries of the International Institute of Refrigeration, Stockholm, Sweden, 2002.
[27] P. Reghem, PhD Thesis. University of Pau, France; 2002.
[28] O. Bel, Contribution a l'etude du comportement thermo-hydraulique d'un melange diphasique dans une boucle frigorifique a stockage d'energie. PhD Thesis. L'Institut National des Sciences Appliquees de Lyon; 1996.
[29] K.G. Christensen, M. Kauffeld, Heat transfer measurements with ice slurry, Conference of the International Institute of Refrigeration, Comission B1, 1997.
[30] J. Bellas, et al., Heat transfer and pressure drop of ice slurries in plate heat exchangers, J Appl Thermal Engng 22 (7) (2002) 721–773.
[31] P.W. Egolf, et al., Pressure drop and heat transfer in a cylindrical heat exchanger with ice slurry flow, Third Workshop on Ice Slurries of the International Institute of Refrigeration, Lucerne, Switzerland, 2001 p. 77–84.
[32] E.J. Wasp, Solid–liquid flow, slurry pipeline transportation, Series on bulk material handlings, vol. 1(4) 1977.
[33] E.N. Jensen, et al., Pressure drop and heat transfer with ice slurry, Conference of the International Institute of Refrigeration, Purdue, USA, 2000.
[34] R.M. Turian, et al., Settling and rheology of suspensions of narrow-sized coal particles, AIChE J 38 (7) (1992) 969–987.
[35] A. Sellgren, Hydraulic behaviour of ice particles in water, Hydrotransport 10 (1986) 213–217.
[36] Takahashi, et al., A laboratory study of pressure loss and pressure fluctuation for ice-water slurry flows in a horizontal pipe, Hydrotransport 12 (1993) 497–511.
[37] O. Sari, D. Vuarnoz, F. Meili, P.W. Egolf, Visualization of ice slurries and ice slurry flows, Second Workshop on Ice Slurries, Paris, 2000 p. 68–80.
[38] D. Vuarnoz, F. Meili, Ph. Moser, O. Sari, P.W. Egolf, Fluid and flow visualizations of ice slurries, Eureka Project FIFE, Research report No. 8, University of Applied Sciences of Switzerland, 2000.
[39] T.M. Hansen, M. Radosevic, M. Kauffeld, Behavior of ice slurry in thermal storage systems, ASHRAE Research Project 1166, ASHRAE, 2002.
[40] M. Kawaji, et al., Ice slurry flow and heat transfer characteristics in vertical rectangular channels and simulation of mixing in a storage tank, Fourth Workshop on Ice Slurries of the International Institute of Refrigeration, Osaka, 2001 p. 153–64.
[41] E. Stamatiou, M. Kawaji, V. Goldstein, Ice fraction measurements in ice slurry flow through a vertical rectangular channel heated from one side, Fifth Workshop on Ice Slurries of the International Institute of Refrigeration, Stockholm, Sweden, 2002.
[42] A. Kitanovski, A. Poredoš, Theory on concentration distribution of the ice slurry flow, Fourth Workshop on Ice Slurries, Osaka, 2001 p. 15–24.
[43] A. Kitanovski, A. Poredoš, Concentration distribution and viscosity of ice slurry in heterogeneous flow, IIR J 25 (6) (2002) 827–835.
[44] Takahashi, et al., Flow properties for slurries of particles with densities close to that of water, ASME, Liquid–Solid Flows 118 (1991) 103–108.
[45] M. Sasaki, Dynamics of snow-water flow in pipelines, Hydrotransport 12 (1993) 535–543.
[46] A. Kitanovski, et al., Flow patterns of ice slurry flows, Fifth Workshop on Ice Slurries of the International Institute of Refrigeration, Stockholm, Sweden 2002.
[47] P. Doron, D. Granica, D. Barnea, Slurry flow in horizontal pipes-experimental and modeling, Int J Multiphase Flow 13 (4) (1987) 535–547.
[48] H. Nasr-El-Din, C.A. Shook, The lateral variation of solid concentration in horizontal slurry pipeline flow, Int J Multiphase Flow 13 (5) (1987) 661–670.
[49] J.F. Richardson, W.N. Zaki, Sedimentation and fliudisation: PART 1, Trans Inst Chem Engng 32 (1954) 35–53.
[50] R.A. Bagnold, Experiments on a gravity-free dispersion of large solid spheres in a Newtonian fluid under shear, Proc R Soc A225 (1954) 49–63.
[51] M.C. Roco, C.A. Shook, New approach to predict concentration distribution in fine particle slurry flows, PCH 8 (1) (1987) 43–60.
[52] C.A. Shook, M.C. Roco, Slurry Flow-Principles and Practice, Butterworth-Heinemann, 1991.
[53] T.C. Papanastasiou, Flows of materials with yield, J Rheol 31 (5) (1987) 385–404.
[54] B.M.A. Lakhdar, Comportement thermohydraulique d'un fluide frigoporteur diphasique: le coulis de glace. PhD Thesis. INSA-Lyon; 1998.